Basin-Scale Assessment of Operational Base Flow Separation Methods

T. A. Stadnyk, M.ASCE[1]; J. J. Gibson[2]; and F. J. Longstaffe[3]

Abstract: Base flow recession analysis is required to estimate the long-term, reliable component of the hydrograph and water cycle, and for drought management, inflow design and analysis, and contaminant and nutrient transport. Operationally, recursive digital filtering (RDF) techniques are commonly applied; however, questions have been raised about the reliability and parameterization of these methods. A comparison of three base flow separation methods, including two popular RDFs and one hydrologic model, is performed in two base flow-dominant subbasins of the Grand River Basin in southern Ontario, Canada. The Eramosa River and Whiteman's Creek subbasins are similar in size (236 and 383 km^2, respectively) and have similar annual runoff distributions yet significantly different physiography governing runoff generation. Subbasin physiographic characteristics are found to result in significant differences in annual base flow distributions, which are well captured by the hydrologic model but not by the RDFs. Stable water isotopes (SWIs) are applied for verification of base flow separations using two-component mixing model separations and show better visual agreement with a base flow derived from the hydrologic model over the RDF methods. Limitations include insufficient isotope data to quantify a statistically significant model fit and results that are tied to subbasin physiography and basin-specific processes. Results support the application of SWIs for regional hydrograph separation and highlight the need for more efficient, yet physically based base flow separation in regions with complex physiography. **DOI: 10.1061/(ASCE)HE.1943-5584.0001089.** *© 2014 American Society of Civil Engineers.*

Author keywords: Base flow; Flow separation; Hydrograph separation; Isotope tracers; Flow tracers.

Introduction

In the field of water resources science and engineering, partitioning of hydrograph components, particularly base flow, is required for drought estimation, inflow prediction, water resources management, and nutrient or contaminant transport. More recently, base flow estimation under climate change has emerged as an important consideration in long-term water use studies, particularly in glacial or snowmelt-dominated basins where climate change is already being experienced (Fan et al. 2013). In the past decade, more studies have been devoted to quantifying base flow time series for environmental issues and conservation studies (Fiorotto and Caroni 2013; Li et al. 2013). The application of graphical recession curve analysis to estimate low-flow contributions is decades old and has evolved into the application of a variety of recursive digital filtering (RDF) algorithms because of their ease of implementation and minimal input requirements (Li et al. 2013; Arnold et al. 1995; Nathan and McMahon 1990). Base flow separation has since evolved to include more complex and computationally intensive methods capable of accounting for regional differences in geology, land cover, and basin physiography (Nejadhashemi et al. 2008; Longobardi and Villani 2008). Integration of base flow separation into hydrologic models ranging from lumped, conceptual, to fully integrated groundwater and surface water simulations has resulted in the opportunity to provide secondary model calibration in ungauged basins where groundwater or tracer data exist (Ahiablame et al. 2013; Samuel et al. 2012).

Over 40 different methods of base flow separation were reviewed and documented by Nejadhashemi et al. (2003), with five methods identified as the top performers with the lowest input data requirements (Nejadhashemi et al. 2008). Among these five were the BFLOW (Nathan and McMahon 1990; Arnold et al. 1995) and HYSEP (Sloto and Crouse 1996) recursive digital filter (RDF) methods. Eckhardt (2008) found the performance of BFLOW and the Eckhardt method (Eckhardt 2005) to be most similar and hydrologically plausible relative to other methods, which tended to linearly interpolate between low-flow sections of the discharge record. All of the above methods require the estimation of parameters or coefficients, which are often difficult (if not impossible) to derive with a physical basis and do not account for regional (spatial) variability. Chapman (1999) highlighted that, when one-, two-, and three-parameter distributions were applied, base flow flow index (BFI) varied substantially and parameter selection was subjective. To address this concern, Collischonn and Fan (2013) proposed a method based solely on discharge records to assist with the estimation of the BFI_{max} parameter (maximum value of the base flow index, or percent base flow) in the Eckhardt model (with a similar parameter in BFLOW), which is typically derived a priori with no physical or quantitative basis. Similar studies have sought to address the shortcomings of RDF methods by estimating optimal parameter values through relationships with catchment physiographic characteristics (Li et al. 2013; Corzo et al. 2007). In contrast, Romanowicz (2010) developed a statistically based low-flow separation model that uses a log-transform approach that essentially decomposes hydrographs into fast (runoff) and slow (base flow) components based on a rate-of-change analysis. Several studies have attempted to estimate base flow using mass-balance models,

[1]Assistant Professor, Dept. of Civil Engineering, Univ. of Manitoba, 15 Gillson St., Winnipeg, MB, Canada R3T 5V6 (corresponding author). E-mail: stadnykt@cc.umanitoba.ca

[2]Research Professor, Water Team Lead, Alberta Innovates Technology Futures, 3-4476 Markham St., Victoria, BC, Canada V8Z 7X8.

[3]Professor, Dept. Earth Sciences, Univ. of Western Ontario, 1151 Richmond St. N, London, ON, Canada N6A 5B7.

Note. This manuscript was submitted on December 8, 2013; approved on August 27, 2014; published online on October 6, 2014. Discussion period open until March 6, 2015; separate discussions must be submitted for individual papers. This paper is part of the ***Journal of Hydrologic Engineering***, © ASCE, ISSN 1084-0699/04014074(11)/$25.00.

but at the cost of more intensive data requirements and parameter estimations (O'Brien et al. 2013; Furey and Gupta 2001).

Hydrograph separation has also been integrated into several hydrologic models ranging from lumped, conceptual, and mass balance (Ferket et al. 2010; Zhang et al. 2013) to distributed, more physically based models such as WATFLOOD (Stadnyk-Falcone 2008), InHM (Sudicky et al. 2008) and others (Hofmann 2013). However, more accurate, physically based methods increase computational effort and input data requirements, thereby limiting their use in data-sparse regions or for regional, operational-based applications. Because of inaccuracies in input data (i.e., precipitation) over larger domains, however, modeled base flow estimations can exceed total streamflow if not constrained within the models. Therefore, despite shortcomings, RDFs are still commonly applied in operational water resource applications because of their ease of use and reliance on discharge records alone. Given the variety of methods and parameters involved, base flow estimation uncertainty can become significant. Hubbart and Zell (2013) recently quantified base flow estimation uncertainty associated with rainfall-runoff relationships, algorithm structure, and model parameterization using a Monte Carlo approach, finding median differences in base flow estimation of upward of 29%. They recommended, in the absence of verification data or direct tracer measurement, that uncertainty analyses should be conducted.

Uncertainty in conventional RDF methods arises when parameters (and base flow estimates) are fit using a low-flow hydrograph recession curve analysis. Depending on the catchment, low flow can be derived from sources other than what is conventionally considered base flow, such as glacial melt or wetland runoff contributions. It is important to distinguish such components from base flow when performing nutrient or contaminant transport modeling, environmental assessments, or long-term water use and allocation studies. Tracer-based studies have also emerged in an attempt to quantify base flow uncertainty and assist with model calibration (Unland et al. 2013; Gonzales et al. 2009; Ribolzi et al. 2000), with the caveat that surface flow chemical compositions need to be known, identifiable, and constant. Since the late 1970s, stable water isotope (SWI) tracers have been used as base flow tracers given their ubiquitous nature and the distinct labeling that arises from isotopic separation between surface (event-based) and subsurface (old water) contributions to the hydrograph (Carey et al. 2013; Munyaneza et al. 2012; Tetzlaff et al. 2009; Brassard et al. 2000; Sklash and Farvolden 1979). Kolka et al. (2010) applied SWIs in conjunction with other geochemical tracers within a riparian-influenced hydrologic regime and found that snowmelt significantly affected subsurface storage and seasonal base flow contributions. Significant spatial and temporal variability was found in base flow contributions.

Hydrologic complexity in regions with significant seasonality (Canada, for example) and variable base flow component contributions (from wetlands, for example) result in significant uncertainties in conventional RDF methods of base flow separation. This study compares two popular RDF methods (HYSEP and BFLOW) with a computationally efficient, partially physically based hydrologic model (WATFLOOD) to perform base flow separation in two base flow-dominant subbasins of southern Ontario's Grand River Basin (GRB). The hydrologic plausibility of all methods is evaluated and their relative correctness tested using SWI mixing-model base flow separations. The objectives of this study are to (1) determine the most practical and accurate method of base flow separation that is still feasible for operational use in water resource engineering applications, and (2) evaluate an SWI tracer method for regional hydrograph separation and hydrologic verification.

Study Site

The Grand River Basin lies between Georgian Bay (Lake Huron) and Lake Erie, stretching from Dundalk, Ontario in the north to Dunnville, Ontario, in the south (Fig. 1), and is located approximately 100 km west of Toronto, Ontario, Canada. It is southern Ontario's largest watershed, with a drainage area of over 6,000 km^2. The headwaters (525 masl) originate in the Dundalk and the Grand Valley regions, with basin elevation decreasing in a southeasterly direction where the Grand River drains into Lake Erie (100 masl) at Port Maitland, approximately 128 km south of the headwater (straight-line distance). The watershed contains four major tributaries: the Conestogo (~800 km^2), Speed (~750 km^2), Nith (1,030 km^2), and Eramosa (~230 km^2) rivers. The GRB has a humid climate (typical continental climate modified by the Great Lakes) and high precipitation (850–1,000 mm annually) with the highest amounts in the northwest, decreasing to the southeast. Rainfall accounts for 80% of the annual precipitation and typically occurs in late summer and early fall. Snow cover typically persists from January to the end of April, where snowfalls can reach depths of 250 cm/year on average in the snow-belt region (northwest) (Environment Canada 2004). The headwater region located to the north in the Dundalk Uplands is cooler with more precipitation falling as snow than rain. In the midbasin region there is a band of higher precipitation, particularly toward the west and southwest, with a milder, drier climate developing southward moving toward Lake Erie (Ivey 2002). Snowmelt hydrographs typically show more than one distinct freshet owing to the temperate southern climate, with peak flow typically in April. Annual minimum discharge occurs in winter when small tributaries are completely ice covered and main tributaries are at least partially ice covered. Peak summer flow results from large convective storm events interspersed with prolonged dry periods with substantial evaporation.

This study focuses on two base flow-dominated subbasins of the GRB at Water Survey of Canada (WSC) gauges: 02GA029, on the Eramosa River at Guelph (236 km^2); and 02GB008, on Whiteman's Creek near Mount Vernon (383 km^2) near Brantford, Ontario, Canada (Table 1). These specific subbasins where chosen because they have simultaneous isotope and hydrometric data and near-identical runoff generation (Fig. 2) based on flow per unit area of watershed, but they are separated by approximately 50 km and have significantly different physiographic features (Table 2). The Eramosa River is largely fed by the Galt and Paris Moraines along the eastern portion of the GRB, composed of thick till deposits and large areas of disconnected drainage with higher wetland coverage (12%). Whiteman's Creek is an ecologically significant cold-water course located in the Norfolk Sand Plains in southern GRB consisting o f a relatively thin deposit of sand and flat topography with 0% wetland coverage. This hydrogeologic variability results in different basin drainage and base flow generation mechanisms, suggesting that although total runoff is similar, base flow percentage may not be.

Methodology

Two methods commonly applied for regional-scale operational base flow separation (i.e., HYSEP and BFLOW) are compared to a partially physically based base flow separation from the WATFLOOD tracer module (Stadnyk-Falcone 2008). This study is intended to provide a basin-scale comparison and an assessment of base flow separation. Direct validation using piezometric base flow was not available, nor would it have been practical for regional studies. The SWIs in the streamflow were used to perform old (base flow) and new (rainfall, snowmelt) water separations for verification purposes. Methods used for base flow separation are explained below.

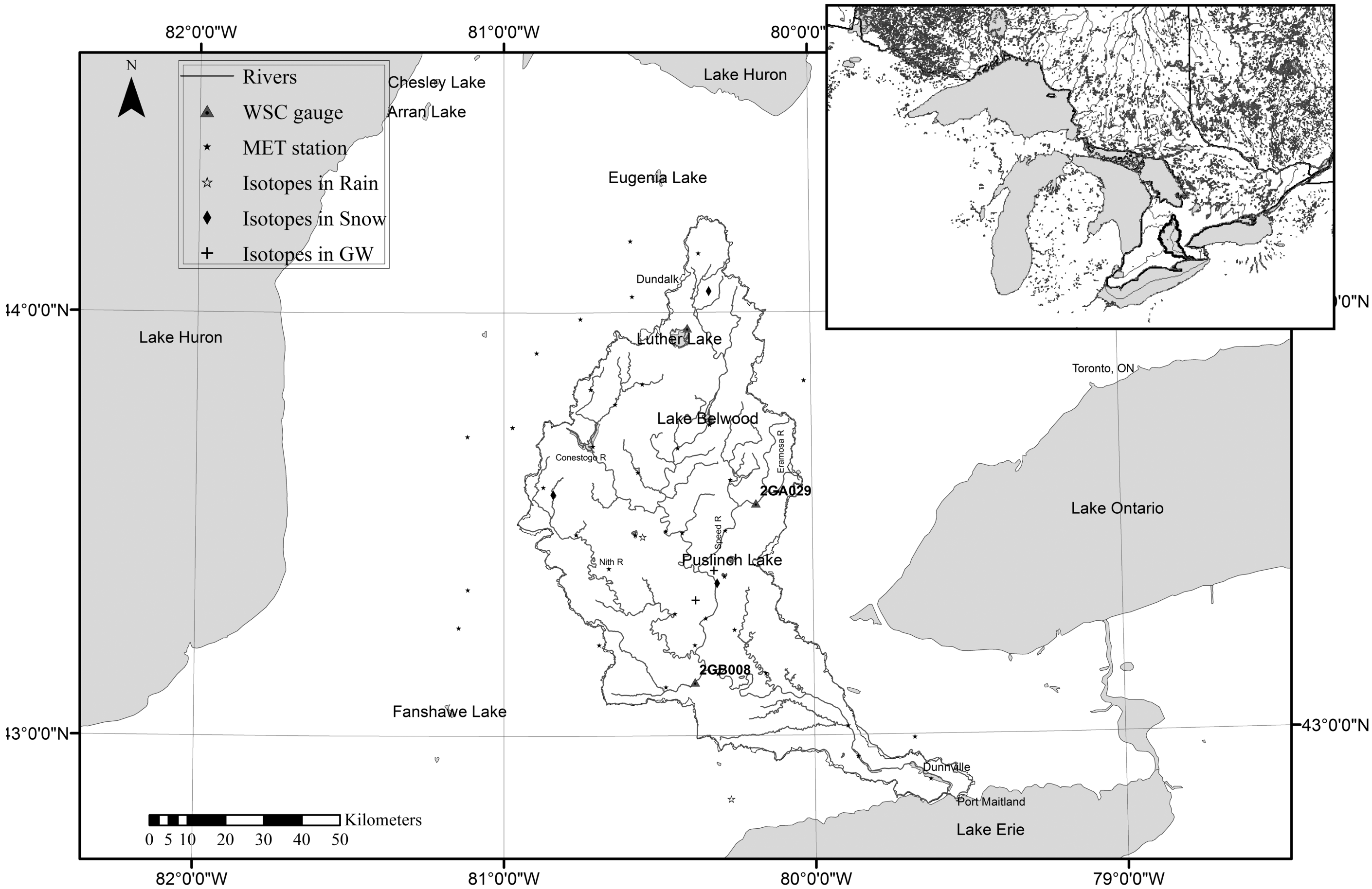

Fig. 1. Grand River Basin, southern Ontario, Canada, showing hydrometric gauge locations for two subbasins of interest and isotope sampling network. [Canadian Council on Geomatics (2014), uses information licensed under the Open Government Licence, Canada (http://data.gc.ca/eng/open-government-licence-canada)]

Table 1. Hydrometric Gauge IDs, Names, and Locations and Locations of Snow, Groundwater, and Isotopes in Precipitation Sampling

WSC[a], PWQMIN[a], or CNIP[b] identifier	Description	Latitude (degrees)	Longitude (degrees)	Average annual flow (m^3/s) or precipitation[c] (cm) or depth to water table[d] (m)
02GA029, 16018410202	Eramosa River at Guelph	43.55	−80.18	2.5
02GB008, 16018410602	Whiteman's Creek near Mount Vernon	43.13	−80.38	4.4
11	Precipitation, Egbert (CNIP)	44.23	−79.77	6.81
28	Precipitation, Simcoe (CNIP)	42.85	−80.27	7.61
Independent gauge	Precipitation, Waterloo (independent)	43.47	−80.55	6.67
Independent gauge	Snow, Cambridge	43.36	−80.31	73
Independent gauge	Snow, Jessopville	44.05	−80.33	60
Independent gauge	Snow, Millbank	43.57	−80.84	108
Independent gauge	Groundwater, Long Point	42.55	−80.06	0–20
Independent gauge	Groundwater, Dryden	43.39	−80.32	0–20
Independent gauge	Groundwater, North Dumfries	43.32	−80.38	0–20

[a]Water Survey of Canada (WSC) hydrometric stations overlap with Provincial Water Quality Monitoring Network (PWQMIN) stations where isotopes in streamflow were collected.
[b]Canadian Network for Isotopes in Precipitation (CNIP) station identifier indicates locations where precipitation was sampled and used to derive δP for mixing models.
[c]Average liquid rainfall or solid (snowfall) over the duration of record used to estimate flux-weighted δP or δS compositions for mixing models.
[d]Average depth to the water table at groundwater sampling locations based on GRCA (2013a, b).

HYSEP

HYSEP is a base flow separation program developed by the USGS (Sloto and Crouse 1996). The RDF separates base flow (low-flow) components from surface runoff (peak flow) based on analysis of a daily observed hydrograph. The duration of surface runoff is estimated from an empirical relationship (Linsley et al. 1982)

$$N = \text{Area}^{0.2} \tag{1}$$

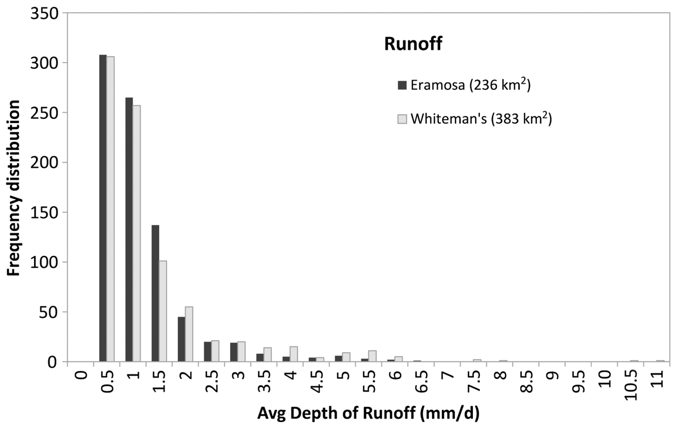

Fig. 2. Distribution of daily observed runoff (in mm) for Eramosa River (02GA029) and Whiteman's Creek (02GB008) subbasins of the GRB

where N = number of days after surface runoff ceases (the interval length); and Area is the drainage area in square miles. The interval ($2N^*$) used for base flow hydrograph separation is defined as the nearest odd integer between 3 and 11 nearest to $2N$ (Pettyjohn and Henning 1979). Three methods are used to determine the lowest flow during an interval: fixed interval, sliding interval, and local minimum (Sloto and Crouse 1996).

Using each basin's drainage area, for a minimum interval length of $2N^*$ equal to 5 was computed for both subbasins, and HYSEP algorithms were run using observed flow at both WSC hydrometric gauges (02GA029 and 02GB008). The fixed and sliding interval and local minimum methods produced very similar results with imperceptible differences in the log scale. However, when the algorithm was applied using the $2N^*$ equal to the 5-day interval, unrealistically high (peaky) and flashy estimations of base flow resulted. Therefore the interval length was increased up to 21 days to produce a lower, more smoothed base flow response (comparable to that of the BFLOW model) that was hydrologically more plausible. The choice of a 21-day interval indicates a significant amount of attenuation in these basins, with a wider, less flashy hydrographic response. The sliding-21 method was chosen for the HYSEP model in this study as providing the most comparable base flow response to the BFLOW and WATFLOOD models relative to the fixed and local-minimum methods.

BFLOW

The BFLOW program is an empirical method of base flow estimation originally developed for the soil water assessment tool (SWAT) and supported by the Soil and Water Research Laboratory, USDA Agricultural Research Service. Base flow is segregated by recursively passing a digital filter over a daily observed flow record. The RDF was originally used in signal analysis and separates low-frequency base flow from high-frequency quick flow (Nathan and McMahon 1990), but it has no physical basis in groundwater flow theory (Arnold and Allen 1999). A filter parameter (β) affects the attenuation of base flow and was determined to range from 0.9 to 0.95; optimally $\beta = 0.925$ (Nathan and McMahon 1990; Arnold et al. 1995). The filter is passed three consecutive times over the streamflow record: forward, backward, and forward again (BFLOW-1, BFLOW-2, and BFLOW-3, respectively). Each successive pass has the effect of lowering and smoothing the estimate of the base flow; the user selects the optimum pass based on knowledge of the catchment and typical base flow recession curves, which for this study was determined to be BFLOW-3. Parameters used for the BFLOW model are summarized in Table 3 and were derived from catchment characteristics and Arnold et al. (1995). Note that the value of alpha (α), the base flow recession parameter, is small, indicating slow drainage and lots of storage. The BFLOW-1 and BFLOW-2 filter passes each produced a very flashy and peaky base flow response, which is not considered to be an expected or realistic base flow response for either subbasin.

WATFLOOD

The WATFLOOD hydrologic model was developed at the University of Waterloo over the past 30 years (http://www.watflood.ca) and is a fully distributed, partially physically based mesoscale hydrologic model for watersheds having response times larger than one hour (Kouwen 2012). The model has been used operationally by hydroelectric utilities and conservation authorities because of its minimal data requirements and quick computation times. A tracer module integrated into WATFLOOD segregates contributions to total streamflow (Stadnyk-Falcone 2008) at their origin, tracking them through the hydrologic cycle. Base flow separation is accomplished through simplified storage routing of responsive groundwater (i.e., base flow) through the subsurface based on a specified concentration of tracer added to the base flow component at its origin. When wetlands are present, the tracer mass is routed twice: once through the wetland and again in streamflow. Because wetlands in WATFLOOD represent riparian zones directly interacting with streamflow (i.e., channelized fens), the mathematics of tracer mass routing in wetlands are not significantly different from channel routing. When upstream lakes are present, tracer mass is accumulated in the lake, routed through the lake minus losses (i.e., evaporation), and tracer outflow computed (governed by a stage-discharge relationship). To prevent base flow from exceeding total flow because of a numerical error caused by the instantaneous mixing assumption within a grid, a retardation coefficient is applied to the tracer mass outflow based on a dispersion coefficient (D^*) computed using the Péclet number (Stadnyk-Falcone 2008).

Simulated hourly hydrographs and base flow separations were generated for 41 hydrometric gauges in the GRB from October 1, 2003, to December 31, 2005. Results for the two gauges of interest (with corresponding hydrometric and isotope data) were averaged daily, and the base flow percentage was computed for each day. The WATFLOOD GRB model was originally calibrated for 1993 using hydrometric records and was recalibrated for 2004–2005 using a coupled-isotope hydrometric approach via the iso-WATFLOOD model (Stadnyk et al. 2013; Stadnyk-Falcone 2008) utilizing river isotope data. This approach significantly reduces the plausible range for end member (i.e., base flow) contributions (i.e., parameterizations) by additionally constraining model degrees of freedom, effectively reducing equifinality (Stadnyk et al. 2005;

Table 2. Land Cover and Basin Physiography for Eramosa River (02GA029) and Whiteman's Creek (02GB008) Subbasins

			Land cover classification (%)						
Basin	Drainage area (km^2)	Slope (%)	Bare	Forest	Agriculture	Bog	Fen	Water	Impervious
Eramosa River	236	0.27	2	23	63	9	3	0	0
Whiteman's Creek	383	0.19	3	11	85	0	0	1	0

Table 3. BFLOW Basin-Specific Input Parameters

Parameter	Eramosa River	Whiteman's Creek	Value
Ndmin	10	10	Default
Ndmax	300	300	Default
Base flow FR1	0.67	0.67	Default
Base flow FR2	0.53	0.53	Default
Base flow FR3	0.46	0.46	Default
NPR	2	2	Record-defined
Alpha	0.0357	0.0134	$= 1/N^* \ln(Q_n/Q_o)$
Base flow days	45	50	Record-defined

Beven and Binley 1992). The outcome may lead to lower overall simulation statistics (relative to what is achievable by hydrometric data alone), but emphasis in the coupled calibration approach is placed on more physically realistic contributions of each end member. The model was considered to be adequately calibrated and representative of long-term flow and base flow percent contribution in the two subbasins despite the simulations not perfectly reproducing observed streamflow at all hydrometric gauge locations. Because observed records were used by HYSEP and BFLOW but WATFLOOD separations were relative to simulated flow, percent daily base flow was used for comparison among the methods. Despite the error inherent in WATFLOOD simulated hydrographs, simulated flows were consistent between the two subbasins and exhibited generally the same runoff distribution (Fig. 3), consistent with the observed runoff (Fig. 2). Whiteman's Creek has more runoff events exceeding 3.5 mm/day than the Eramosa River (Fig. 3), which is anticipated because of the creek's more western location (i.e., higher precipitation). For time series validation, the percent WATFLOOD-simulated base flow was multiplied by observed flow to produce a time series of base flow that could be directly compared with BFLOW-3 and HYSEP sliding-21 separations.

Isotope Mass Balance

Stable water isotope data (δ^{18}O and δ^2H) was available at the gauges of interest over the study period (2003–2005) and partitioned using two-component mixing models to estimate base flow for verification purposes. As part of the Grand River isotope sampling initiative, snow ($n = 22$) and groundwater ($n = 90$) samples were collected at various locations throughout the GRB during the study period (Fig. 1, Table 1), enabling flux-weighted average values of C_S (snow) and C_{GW} (ice-on, low flow) to be estimated ($-17.1‰\delta^{18}$O, $-121‰\delta^2$H; $-10.5‰\delta^{18}$O, $-70.5‰\delta^2$H, respectively) along with their standard deviations (3.3‰ and 26‰, respectively). Isotopes in precipitation were not collected as part of the sampling program, but two Canadian Network for Isotopes in Precipitation (CNIP) stations (Simcoe and Egbert) were located nearby and were used to compute long-term average compositions ($-9.15‰\delta^{18}$O and $-61.2‰\delta^2$H) and standard deviations (0.60‰ and 4.6‰, respectively). Isotopes in precipitation data were also available from a University of Waterloo weather station, although outside the study period (2001), and were used to verify consistency of the isotope in the precipitation signal across the GRB and to ensure appropriateness of the long-term average computed from the CNIP stations.

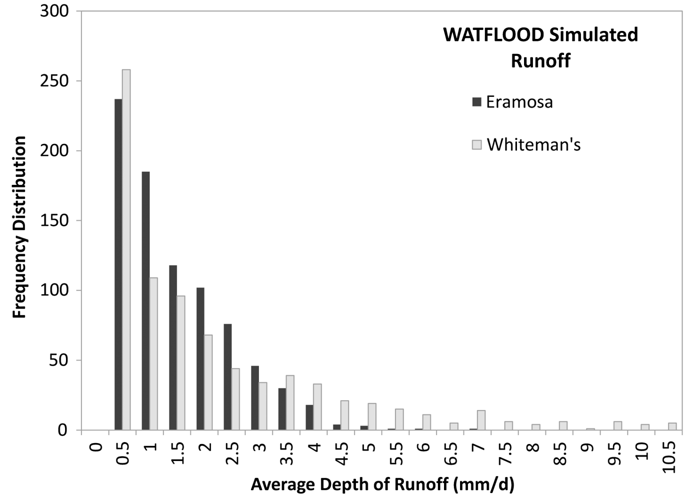

Fig. 3. Distribution of daily runoff simulated by WATFLOOD (in mm per basin area) for Eramosa River (02GA029) and Whiteman's Creek (02GB008) subbasins of the GRB

A two-component mixing model separation of "old" (base flow) and "new" (surface water) components was performed for ice-off periods when isotope data were available. Separations were made using both stable isotopes (δ^{18}O and δ^2H) and following the procedure described by St. Amour et al. (2005). Separations of base flow are dependent on the differences between isotopic compositions of source waters (i.e., surface water, C_{SW}, and groundwater, C_{GW}) and streamflow (measured, C_Q). It is generally accepted that the more separation there is between components, the more accurate the estimations (St. Amour et al. 2005). Given that isotopic separations were applied as a means of base flow verification, uncertainty in the base flow component (W_G) was computed using the procedure described by Genereux (1998) and Eq. (2)

$$W_G = \sqrt{\left[\frac{C_{\mathrm{SW}} - C_Q}{(C_{\mathrm{GW}} - C_{\mathrm{SW}})^2} W_{\mathrm{CGW}}\right]^2 + \left[\frac{C_Q - C_{\mathrm{GW}}}{(C_{\mathrm{GW}} - C_{\mathrm{SW}})^2} W_{\mathrm{CSW}}\right]^2 + \left(\frac{1}{C_{\mathrm{GW}} - C_{\mathrm{SW}}} W_{\mathrm{CQ}}\right)^2} \quad (2)$$

where W_{CGW}, W_{CSW}, and W_{CQ} = uncertainty in groundwater, surface, and streamflow components, respectively. Component uncertainty was computed as the analytical uncertainty ($0.1‰\delta^{18}$O, $2‰\delta^2$H) plus the standard deviation of each component. Table 4 summarizes the percent maximum surface water, surface water, groundwater, and uncertainty in groundwater derived from the isotope data.

Average base flow for the Eramosa River was estimated between 70–80% with 15–18% uncertainty and 61–78% for Whiteman's Creek with 14–18% uncertainty. Base flow compositions during ice-off periods derived in this study are similar to those derived by others (St. Amour et al. 2005; Kolka et al. 2010; Jeelani et al. 2013). Base flow compositions using isotope-based mixing models tend to be high because they compute total "old" water

Table 4. Isotopic Base Flow Separations Based on Seasonal Two-Component Mixing Model

	Maximum surface water R_{SW} (%)		Average surface water R_{SW} (%)		Average base flow R_{GW} (%)		Uncertainty (%)	
Basin	$\delta^{18}O$	δ^2H	$\delta^{18}O$	δ^2H	$\delta^{18}O$	δ^2H	$\delta^{18}O$	δ^2H
Eramosa River	98	67	32	21	70	80	15	18
Whiteman's Creek	100	100	36	19	61	78	14	18

Note: Uncertainty based on Genereux (1998) and includes analytical uncertainty in component separations.

(i.e., soil water) contributions relative to new or event-based (i.e., rainfall) contributions. This was considered accurate for this study because the RDF algorithms compute the same quantity, finding and connecting the low-flow points from the observed record. Uncertainty in the isotope separations would decrease with the availability of more isotope data over more consistent (and lengthy) time periods; however, uncertainties are similar to those reported in the literature (Carey et al. 2013; St. Amour et al. 2005) and are considered adequate for verification. Averages of the $\delta^{18}O$ and δ^2H separations were taken to arrive at a single base flow percentage for verification purposes. Unlike the algorithms, isotope separations were not continuous and were only performed when river isotope samples were taken. Statistical comparisons for validation were therefore only made based on dates with isotope data ($n = 14$ for Eramosa, $n = 40$ for Whiteman's Creek).

Results and Discussion

Comparisons of the HYSEP sliding-21, BFLOW-3, and WATFLOOD methods were made to assess the suitability and accuracy of regional base flow estimation for the Eramosa River and Whiteman's Creek subbasins. Figs. 4(a and b) compare the fraction of base flow computed by the HYSEP sliding-21 method [i.e., proportion of base flow, or GW(HYSEP) relative to total observed flow, Q_{obs}] to that from BFLOW-3 [GW(BFLOW) relative to total observed flow, Q_{obs}] for the Eramosa River and Whiteman's Creek, respectively. Consistency between the methods is evident with scatter-plot slopes equal to 0.99 for both subbasins (r^2 of 0.92 and 0.95, respectively), with both simulating essentially the same time series of base flow relative to the observed records. However, no significant correlation was found when BFLOW-3 was similarly compared to the time series base flow

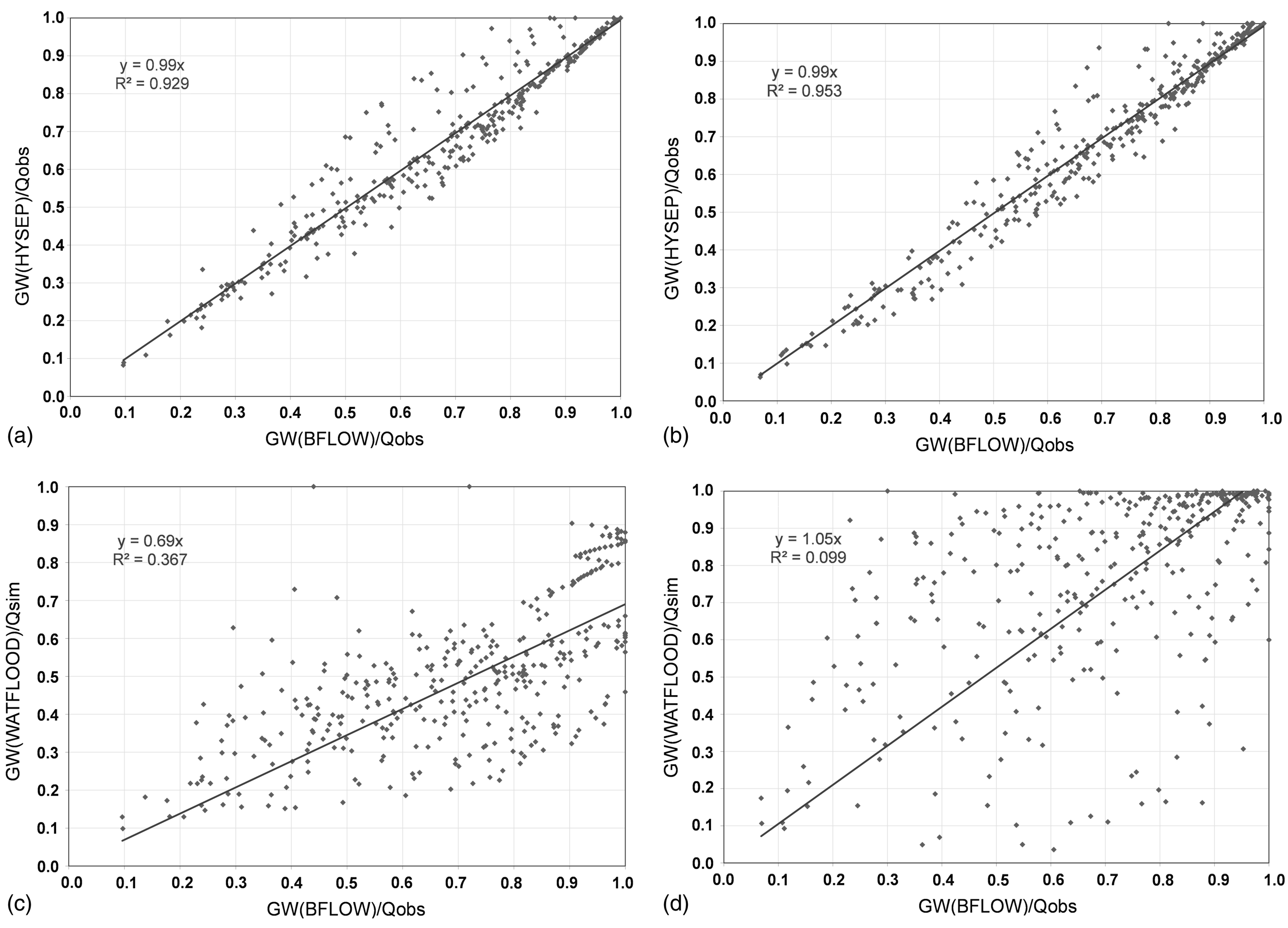

Fig. 4. Comparison of fraction base flow estimations from HYSEP sliding-21 and BFLOW-3 algorithms relative to observed flow for (a) Eramosa River; (b) Whiteman's Creek; and WATFLOOD tracer base flow relative to simulated flow for (c) Eramosa River; (d) Whiteman's Creek

computed by WATFLOOD ($r^2 = 0.36$ and 0.09) [Figs. 4(c and d)]. It was found that WATFLOOD simulates a lower base flow fraction [slope = 0.63, GW(SPL) relative to total simulated flow, Q_{sim}] than the BFLOW (and similarly HYSEP) in the Eramosa River and about the same base flow contribution on average (slope = 1.05) for Whiteman's Creek, but with significant over- and underestimations through time.

Comparing base flow frequency distributions among the algorithms (Fig. 5), the BFLOW and HYSEP algorithms compute nearly the same frequency distribution in the Eramosa River (70% and 69% on average, respectively) and Whiteman's Creek (67% and 66% on average, respectively) with only 1% difference in the standard deviations of the distributions (Table 5). Fig. 5(a) shows, however, that WATFLOOD computes a higher frequency of lower percent base flow fraction in the Eramosa River (46% on average) relative to Whiteman's Creek (74% on average), with the distribution of base flow being normally distributed for the Eramosa River but not in Whiteman's Creek [Fig. 5(b)]. Table 5 shows a relative difference (in percent base flow) between the BFLOW and HYSEP algorithms of +1% and +5% for Eramosa River and Whiteman's Creek, respectively, and probabilities of 41% and 51%, respectively, that the variance between the two base flow time series is not significantly different based on a two-tailed F-test. However, between BFLOW and WATFLOOD the relative differences are −21% and +26% for Eramosa River and Whiteman's Creek, respectively, with 0% and 7.6% probabilities that the variances of the base flow time series are the same. Kolmogorov–Smirnov (KS)

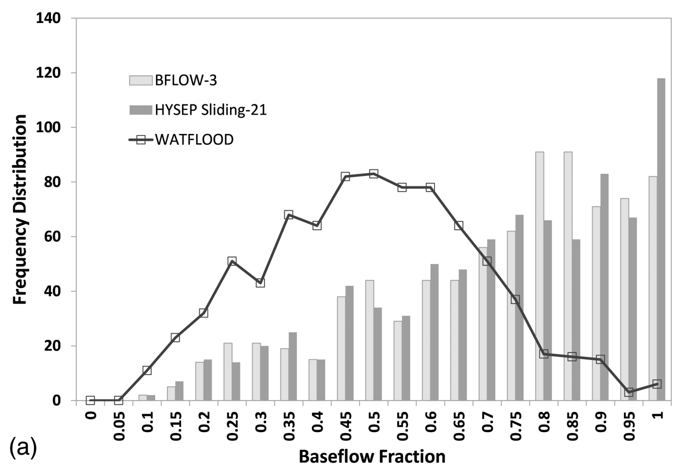

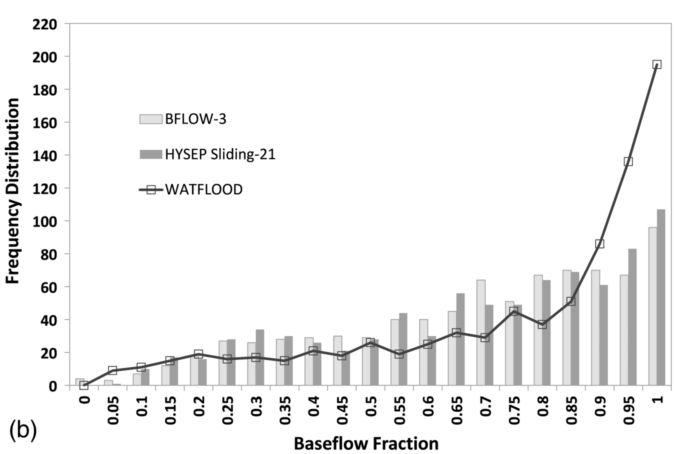

Fig. 5. Base flow distributions (as fraction of total flow) from the BFLOW-3, HYSEP sliding-21, and WATFLOOD algorithms for the (a) Eramosa River; (b) Whiteman's Creek subbasins

tests were performed to discern whether the base flow distributions are statistically similar, with the null hypothesis assuming that the data are from the same continuous distribution (i.e., "0") and a score of "1" indicating that the null hypothesis is rejected at the 95% confidence level. Table 5 confirms, for both subbasins, that the HYSEP and BFLOW distributions are the same, yet BFLOW and WATFLOOD distributions are statistically different. Furthermore, the skewness of the base flow distributions indicates a difference between WATFLOOD (i.e., positive skew) and the two RDF methods (negatively skewed) in the Eramosa River subbasin, but it is in agreement among all three distributions of base flow for Whiteman's Creek (negatively skewed). These results indicate that the BFLOW-3 and HYSEP sliding-21 methods yield the same statistical base flow separations and no differences between subbasins, whereas WATFLOOD is significantly different from the RDF methods and among the subbasins.

Without field data to validate base flow contributions, there is no exact way to determine which of the three (arguably two) separations is most correct. Physiographic differences between the two subbasins suggest, however, that base flow fractions should not be the same between the two study sites, which was only represented by WATFLOOD base flow separations. The SWI data in each subbasin were used to derive tracer-based separations of base flow, which are plotted against time series base flow separations from the BFLOW-3, HYSEP sliding-21, and WATFLOOD methods (relative to total observed flow) (Fig. 6); these results are shown in a log scale to magnify low flows. Note that what appear to be "sudden" changes in WATFLOOD base flow are in fact the result of the log scale; actual changes are more gradual and small in magnitude over time. Error bars on isotopically derived base flow separations are plotted based on the results of the uncertainty analysis (Table 4). Relative to the RDF algorithms, WATFLOOD base flow separations indicate a more variable base flow response, which is generally in better agreement with isotope-based separations (where isotope data were available) that appear to capture both base flow peaks and recessions over time. This characteristic behavior, where base flow is higher following peak flow events, has been noted by Gonzales et al. (2009) and others and is explained as pre-event water being pushed out of storage in a piston-flow-type recharge process. Both RDF methods, by comparison, were much smoother and less variable through time and tended to be in agreement with isotopic separations for median and lower base flow contributions, but not representative of higher base flow contributions. The prediction error reported as the root mean square error (RMSE in m^3/s) in Table 6 for the base flow simulations (relative to isotopic separations) supports this finding for the Eramosa River (0.14 relative to 0.16 for the other methods) and shows little difference among the methods for Whiteman's Creek (<3%). When normalized by average base flow fraction, the RMSE in Whiteman's Creek is lower for WATFLOOD relative to the RDF methods but not statistically different among the methods for the Eramosa River. Note there were insufficient isotope data to plot distributions and compute probabilities of exceedance (or levels of significance).

Examination of the RDF methodologies reveals the reason for consistency among base flow simulations: the methods are designed to find and connect low-flow points among time series flows. On one hand, because both subbasins have near-identical runoff distributions and similar flow records, base flow fractions will also be similar using such types of algorithms. Romanowicz (2010) developed a low-flow separation method that went beyond traditional RDFs by using statistical methods to segregate fast (runoff) and slow (base flow) components of a hydrograph that, once calibrated, could be forced with evaporation and rainfall data to provide more physically based separations. The disadvantage of

Table 5. Statistical Comparison of Base Flow Separations in Percent Base Flow Including Average, Standard Deviation, Minimum, and Maximum Base Flow Fraction

	02GA029 Eramosa River			02GB008 Whiteman's Creek		
Statistical model	HYSEP	BFLOW	WAT	HYSEP	BFLOW	WAT
AVG (%)	70	69	47	67	66	74
STDEV (%)	23	22	19	26	25	27
SKEW	−0.62	−0.69	0.13	−0.59	−0.62	−1.1
MIN (%)	8.2	9.6	5.8	4.2	0.0	2.5
MAX (%)	100	100	100	100	100	100
Relative difference: (HYSEP-BFLOW)/BFLOW	+1		—	+5		—
KS test (95% confidence)	0		—	0		—
F-test (%p)(BFLOW−HYSEP)	41		—	51		—
Relative difference: (SPL−BFLOW)/BFLOW	—	−26		—	+28	
KS test (95% confidence)	—	1		—	1	
F-test (%p) (BFLOW−SPL)	—	0.0		—	7.6	

Note: Relative difference between HYSEP and BFLOW and WATFLOOD and BFLOW are also shown, including percent probability of similarity of the base flow distributions from a standard F-test.

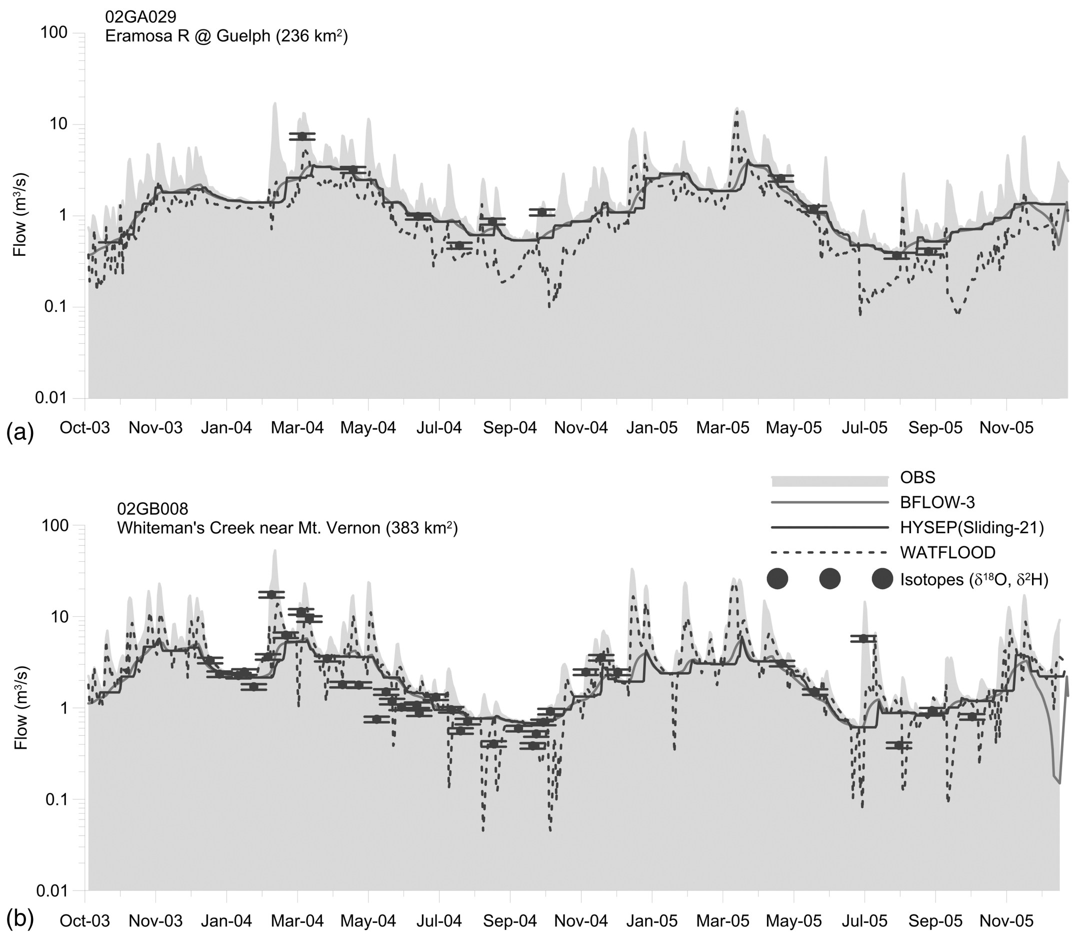

Fig. 6. Time series (in log scale) base flow separations comparing the three methods with isotope-based mixing model separations for (a) Eramosa River at Guelph (236 km^2); (b) Whiteman's Creek near Mt. Vernon (383 km^2)

this approach, however, is that it assumes that all slow flow responses are true base flow and would not be able to detect differences in base flow derived from soil or groundwater from slow-release wetland responses. The WATFLOOD-computed base flow, on the other hand, is computed based on discharge from lower zone storage in the model, which is one component of more detailed water balance and routing modules. The processes and parameters controlling lower zone storage and discharge functions in the model are spatially variable (i.e., by grid) and are determined from digital elevation model (DEM) and land cover inputs that capture physiographic differences (including wetlands). The parameter estimation error was controlled in this study using a coupled isotope-hydrometric approach that more rigorously constrains model parameters (and output). Rigorous and physically based hydrologic model calibration is essential to obtain representative base flow separation, as is proper calibration of the RDF methods (or any model for that matter). In WATFLOOD, low flow generated from wetland discharge is not considered base flow but treated as a

Table 6. Root Mean Square Error (RMSE in m^3/s), Normalized (by Average Flow over the Simulation Period, Q_{bar}) RMSE and Validation Sample Size (n) for the Three Base Flow Separation Methods for Eramosa River and Whiteman's Creek

Relative change from isotope separation	02GA029 Eramosa River			02GB008 Whiteman's Creek		
	HYSEP	BFLOW	WAT	HYSEP	BFLOW	WAT
n (2004)		8			34	
n (2005)		6			6	
RMSE (m^3/s)	0.16	0.16	0.14	0.62	0.62	0.64
RMSE/Q_{bar}	0.11	0.12	0.12	0.28	0.28	0.21

separate contribution to streamflow. This explains the significantly lower contribution of base flow in the Eramosa River (12% wetland) relative to Whiteman's Creek, where 100% of the low flow is derived from base flow (0% wetland). It is because of the differing base flow fractions (representative of basin physiography) that perhaps a higher degree of confidence can be placed on the WATFLOOD simulations in this study. Such differences would have occurred even if the hydrologic model had been calibrated in the traditional sense (i.e., hydrometrically) because of how water is partitioned within the model itself. Higher base flow fractions are anticipated in Whiteman's Creek, which sustains a cold-water trout fishery. In Eramosa River, although low flows are equally as common, they are likely also influenced by wetland-channel dynamics from the significant riparian zone coverage and disconnected drainage network from underlying karst geological formations (GRCA 2013c). It should be noted that because the SWI sampling program was not specifically designed for base flow studies, the lowest flows on record were unfortunately not sampled; thus there is no direct verification of the lowest flow bins.

Conclusions

Three base flow separation algorithms were applied in two subbasins residing in different regions of the GRB in southern Ontario, Canada. The evaluation of algorithm performance is, at this point, specific to this study and the unique physiographic characteristics and differences of this region. Moreover, it is impossible to report whether differences among the base flow separation methods relative to the isotope data are statistically significant given the poor temporal resolution of the isotope data. However, the method applied represents a unique and potentially useful verification for modeled hydrograph separations when traditional, more extensive field studies are not feasible and differences among the RDF schemes and WATFLOOD were notable.

The RDF schemes were consistently in agreement with similar observed flow records and frequencies of low flow. The WATFLOOD-based separations showed distinctly different base flow distributions for Eramosa River (47%, on average) and Whiteman's Creek (74%, on average), resulting from variable runoff partitioning (i.e., governed by model parameters) and governing low-flow processes (i.e., governed by land cover). Physiographic differences between the two subbasins suggest that that there should be differences in base flow fraction between these basins, which are supported by previous studies where differences in land cover, geology, or permeability exist (Kolka et al. 2010; Nejadhashemi et al. 2008; Longobardi and Villani 2008). On a basin-wide scale there is no method of direct measurement to confirm base flow contributions because groundwater monitoring is point-specific, expensive, and time consuming to implement. For larger watersheds, fully integrated groundwater–surface-water models are prohibitive because of input data and parameterization requirements. This study highlights an alternative to RDFs that requires more upfront time investment but yields a more physically based, verifiable base flow separation, assuming that a properly calibrated hydrologic model is achievable and accurately represents partitioning of surface and subsurface flows. Land cover, particularly wetland coverage, was shown to affect base flow partitioning in this study and resulted in spatially (and temporally) variable results. The distinction between low-flow contributions from wetland discharge and base flow is essential for environmental impact, climate change, nutrient management, and contaminant transport studies and should not be disregarded.

Availability of SWIs in the streamflow enabled an indirect verification of base flow in the absence of groundwater data using seasonally applied, two-component mixing model separations. In comparison to the collection of groundwater data, isotope-based separations require significantly less field commitment and expense and can be coupled with existing hydrometric programs (Smith et al. 2014; Kendall and Coplen 2001). Lower temporal resolution and inconsistency in sampling methodology resulted in higher uncertainty and an inability to quantify statistical significance for base flow distributions. The SWI sampling program in the GRB was not designed with the specific goal of base flow separation; however, the presence of the tracer data was shown to be valuable to this study. Future studies utilizing SWIs for base flow separation should have greater temporal resolution and specifically target low-flow periods to further validate WATFLOOD-based separations.

Regional-scale applications of SWIs are becoming more common as a result of their ease of collection, relatively low cost, and value to many hydrological applications. Such SWI sampling has previously been integrated with operational hydrometric programs (Smith et al. 2014; Yi et al. 2012; Kendall and Coplen 2001) and is currently being piloted in Canada's operational hydrometric network. The international community has similarly recognized the value of SWI tracers, with the International Atomic Energy Agency's Global Network for Isotopes in Rivers initiative promoting the collection of SWI data in large rivers around the world (IAEA 2012). This study serves to highlight the value-added nature of SWIs in the regional and subbasin scale in hydrologic studies.

Acknowledgments

The authors would like to acknowledge the Laboratory for Stable Isotope Science (LSIS) at the University of Western Ontario for analyzing the Grand River isotope samples and all those who were involved with sample collection. We thank our reviewers for greatly improving this manuscript. We would like to thank Dr. Andrew Piggott, Environment Canada, for assistance with coordination of the water sampling. We would also like to thank the Grand River Conservation Authority for initiating the study and Drs. Kouwen and Edwards, who supported the WATFLOOD tracer module development. This is LSIS contribution #310.

References

Ahiablame, L., Chaubey, I., Engel, B., Cherkauer, K., and Merwade, V. (2013). "Estimation of annual baseflow at ungauged sites in Indiana USA." *J. Hydrol.*, 476, 13–27.

Arnold, J. G., and Allen, P. M. (1999). "Automated methods for estimating baseflow and ground water recharge from streamflow records." *J. Am. Water Resour. Assoc.*, 35(2), 411–424.

Arnold, J. G., Allen, P. M., Muttiah, R., and Bernhardt, G. (1995). "Automated base-flow separation and recession analysis techniques." *Ground Water*, 33(6), 1010–1018.
Beven, K., and Binley, A. (1992). "The future of distributed models: Model calibration and uncertainty prediction." *Hydrol. Processes*, 6(3), 279–298.
Brassard, P., Waddington, J. M., Hill, A. R., and Roulet, N. T. (2000). "Modelling groundwater and surface water mixing in a headwater wetland: Implications for hydrograph separation." *Hydrol. Processes*, 14(15), 2697–2710.
Canadian Council on Geomatics. (2014). "Geobase geospatial data." ⟨http://www.geobase.ca/geobase/en/index.html⟩ (Sep. 2, 2014).
Carey, S. K., Boucher, J. L., and Duarte, C. M. (2013). "Inferring groundwater contributions and pathways to streamflow during snowmelt over multiple years in a discontinuous permafrost subarctic environment (Yukon, Canada)." *Hydrogeol. J.*, 21(1), 67–77.
Chapman, T. (1999). "A comparison of algorithms for stream flow recession and baseflow separation." *Hydrol. Processes*, 13(5), 701–714.
Collischonn, W., and Fan, F. M. (2013). "Defining parameters for Eckhardt's digital baseflow filter." *Hydrol. Processes*, 27(18), 2614–2622.
Corzo, G., and Solomatine, D. (2007). "Baseflow separation techniques for modular artificial neural network modelling in flow forecasting." *Hydrol. Sci. J.*, 52(3), 491–507.
Eckhardt, K. (2005). "How to construct recursive digital filters for baseflow separation." *Hydrol. Processes*, 19(2), 507–515.
Eckhardt, K. (2008). "A comparison of baseflow indices, which were calculated with seven different baseflow separation methods." *J. Hydrol.*, 352(1–2), 168–173.
Environment Canada. (2004). *Canadian Climate Normals (1971–2000)*, ⟨http://www.climate.weatheroffice.ec.gc.ca/climate_normals/results_e.html⟩ (Apr. 15, 2008).
Fan, Y., Chen, Y., Liu, Y., and Li, W. (2013). "Variation of baseflows in the headstreams of the Tarim River basin during 1960–2007." *J. Hydrol.*, 487, 98–108.
Ferket, B. V. A., Samain, B., and Pauwels, V. R. N. (2010). "Internal validation of conceptual rainfall-runoff models using baseflow separation." *J. Hydrol.*, 381(1–2), 158–173.
Fiorotto, V., and Caroni, E. (2013). "A new approach to master recession curve analysis." *Hydrol. Sci. J.*, 58(5), 966–975.
Furey, P. R., and Gupta, V. K. (2001). "A physically based filter for separating base flow from stream time series." *Water Resour. Res.*, 37(11), 2709–2722.
Genereux, D. P. (1998). "Quantifying uncertainty in tracer-based hydrograph separations." *Water Resour. Res.*, 34(4), 915–919.
Gonzales, A. L., Nonner, J., Heijkers, J., and Uhlenbrook, S. (2009). "Comparison of different base flow separation methods in a lowland catchment." *Hydrol. Earth Syst. Sci.*, 13(11), 2055–2068.
Grand River Conservation Authority (GRCA). (2013a). "GRCA GIS download tool." ⟨http://grims.grandriver.ca/imf/imf.jsp?site=grca_datadis&ddsid=925285⟩ (Nov. 5, 2013).
Grand River Conservation Authority (GRCA). (2013b). "Long Point region approved updated assessment report." ⟨www.sourcewater.ca⟩ (Nov. 6, 2013).
Grand River Conservation Authority (GRCA). (2013c). "Welcome to the Grand River Watershed, Grand River Conservation Authority." ⟨http://www.grandriver.ca/index.cfm⟩ (Nov. 6, 2013).
Hofmann, H. (2013). "Investigating the spatio-temporal variability in groundwater and surface water interactions: A multi-technique approach." *Hydrol. Earth Syst. Sci.*, 17(9), 3437–3453.
Hubbart, J. A., and Zell, C. (2013). "Considering streamflow trend analyses uncertainty in urbanizing watersheds: A baseflow case study in the central United States." *Earth Interact.*, 17(5), 1–28.
International Atomic Energy Agency (IAEA). (2012). "Monitoring isotopes in rivers: Creation of the global network for isotopes in rivers (GNIR)." *IAEA-TECDOC-1673*, Vienna, Austria, 253.
Ivey, J. (2002). "Grand River watershed characterisation report." Univ. of Guelph, Guelph Water Management Group, Guelph, ON, Canada.
Jeelani, J. H., Kumar, U. S., and Kumar, B. (2013). "Variation of δ18O and δD in precipitation and stream waters across the Kashmir Himalaya (India) to distinguish and estimate the seasonal sources of stream flow." *J. Hydrol.*, 481, 157–165.
Kendall, C., and Coplen, T. B. (2001). "Distribution of oxygen-18 and deuterium in river waters across the United States." *Hydrol. Processes*, 15(7), 1363–1393.
Kolka, R. K., Giardina, C. P., McClure, J. D., Mayer, A., and Jurgensen, M. F. (2010). "Partitioning hydrologic contributions to an 'old-growth' riparian area in the Huron Mountains of Michigan, USA." *Ecohydraulics*, 3(3), 315–324.
Kouwen, N. (2012). *WATFLOOD/WATROUTE hydrological model routing & flood forecasting system: User's manual*, Univ. of Waterloo, Waterloo, ON, Canada.
Li, L., Maier, H. R., Lambert, M. F., Simmons, C. T., and Partington, D. (2013). "Framework for assessing and improving the performance of recursive digital filters for baseflow estimation with application to the Lyne and Hollick filter." *Environ. Modell. Software*, 41, 163–175.
Linsley, R. K., Kohler, M. A., and Paulhus, J. L. (1982). *Hydrology for engineers*, 3rd Ed., McGraw-Hill, New York.
Longobardi, A., and Villani, P. (2008). "Baseflow index regionalization analysis in a Mediterranean area and data scarcity context: Role of the catchment permeability index." *J. Hydrol.*, 355(1–4), 63–75.
Munyaneza, O., Wenninger, J., and Uhlenbrook, S. (2012). "Identification of runoff generation processes using hydrometric and tracer methods in a meso-scale catchment in Rwanda." *Hydrol. Earth Syst. Sci.*, 16(7), 1991–2004.
Nathan, R. J., and McMahon, T. A. (1990). "Evaluation of automated techniques for baseflow and recession analysis." *Water Resour. Res.*, 26(7), 1465–1473.
Nejadhashemi, A. P., Shirmohammadi, A., and Montas, H. J. (2003). "Evaluation of streamflow partitioning methods." *ASAE Paper No. 032183*, American Society of Agricultural and Biological Engineers, St. Joseph, MI.
Nejadhashemi, A. P., Shirmohammadi, A., Montas, H. J., Sheridan, J. M., and Bosch, D. D. (2008). "Watershed physical and hydrological effects on baseflow separation." *J. Hydrol. Eng.*, 10.1061/(ASCE)1084-0699(2008)13:10(971), 971–980.
O'Brien, R. J., Misstear, B. D., Gill, L. W., Deakin, J. L., and O'Brien, R. F. (2013). "Developing an integrated hydrograph separation and lumped modelling approach to quantifying hydrological pathways in Irish river catchments." *J. Hydrol.*, 486, 259–270.
Pettyjohn, W. A., and Henning, R. (1979). "Preliminary estimate of groundwater recharge rates, related streamflow and water quality in Ohio." *Center Project Completion Rep. No. 552*, Ohio State Univ., Water Resources, Columbus, OH, 323.
Ribolzi, O., Andrieux, P., Valles, V., Bouzigues, R., Bariac, T., and Voltz, M. (2000). "Contribution of groundwater and overland flows to storm flow generation in a cultivated Mediterranean catchment. quantification by natural chemical tracing." *J. Hydrol.*, 233(1–4), 241–257.
Romanowicz, R. (2010). "An application of a log-transformed low-flow (LTLF) model to baseflow separation." *Hydrol. Sci. J.*, 55(6), 952–964.
Samuel, J., Coulibaly, P., and Metcalfe, R. A. (2012). "Identification of rainfall-runoff model for improved baseflow estimation in ungauged basins." *Hydrol. Processes*, 26(3), 356–366.
Sklash, M. G., and Farvolden, R. N. (1979). "The role of groundwater in storm runoff." *J. Hydrol.*, 43(1–4), 45–65.
Sloto, R. A., and Crouse, M. Y. (1996). "HYSEP: A computer program for streamflow hydrograph separation and analysis." *Water Resource Investigations No. 96-4040*, USGS, Lemoyne, PA.
Smith, A., Delavau, C., and Stadnyk, T. (2014). "Hydrologic assessment of the lower Nelson River basin using stable isotope distribution." *CWRJ*, #1083, in press.
Stadnyk, T. A., Delavau, C., Kouwen, N., and Edwards, T. W. D. (2013). "Towards hydrological model calibration and validation: Simulation of stable water isotopes using the isoWATFLOOD model." *Hydrol. Processes*, 27(25), 3791–3810.
Stadnyk, T. A., St. Amour, N. A., Kouwen, N., Edwards, T. W. D., Pietroniro, A., and Gibson, J. J. (2005). "A groundwater separation study in boreal wetland terrain: The WATFLOOD hydrological model compared with stable isotope tracers." *Isot. Environ. Health Stud.*, 41(1), 49–68.

Stadnyk-Falcone, T. A. (2008). "Mesoscale hydrological model validation and verification using stable water isotopes: The isoWATFLOOD model." Ph.D. thesis, Univ. of Waterloo, ON, Canada, 385.

St. Amour, N. A., Gibson, J. J., Edwards, T. W. D., Prowse, T. D., and Pietroniro, A. (2005). "Isotopic time-series partitioning of streamflow components in wetland-dominated catchments, lower Liard River basin, northwest territories, Canada." *Hydrol. Processes*, 19(17), 3357–3381.

Sudicky, E. D., Jones, J. P., Park, Y. J., and Brookfield, A. (2008). "Simulating complex flow and transport dynamics in an integrated surface-subsurface modeling framework." *Geosci. J.*, 12(2), 107–122.

Tetzlaff, D., and Soulsby, C. (2009). "Sources of baseflow in larger catchments: Using tracers to develop a holistic understanding of runoff generation." *J. Hydrol.*, 359, 287–302.

Unland, N. P., et al. (2013). "Investigating the spatio-temporal variability in groundwater and surface water interactions: A multi-technique approach." *Hydrol. Earth Syst. Sci.*, 17(9), 3437–3453.

Yi, Y., et al. (2012). "Isotopic signals (18O, 2H, 3H) of six major rivers draining the pan-Arctic watershed." *Global Biogeochem. Cycles*, 26(1), GB1027.

Zhang, R., Li, Q., Chow, L. T., Li, S., and Danielescu, S. (2013). "Baseflow separation in a small watershed in New Brunswick, Canada, using a recursive digital filter calibrated with the conductivity mass balance method." *Hydrol. Processes*, 27(18), 2659–2665.